Syntaxin 17, an ancient SNARE paralog, plays different and conserved roles in different organisms

Shun Kato[1], Kohei Arasaki[1,*], Natsuki Tokutomi[1], Yuzuru Imai[2,3], Tsuyoshi Inoshita[4], Nobutaka Hattori[2,3,4], Taeko Sasaki[5], Miyuki Sato[5], Yuichi Wakana[1], Hiroki Inoue[1] & Mitsuo Tagaya[1,*]

[1]School of Life Sciences, Tokyo University of Pharmacy and Life Sciences, Hachioji, Tokyo 192-0392, Japan

[2]Department of Research for Parkinson's Disease, Juntendo University Graduate School of Medicine, Tokyo 113-8421, Japan

[3]Department of Neurology, Juntendo University School of Medicine, 2-1-1 Hongo, Bunkyo-ku, Tokyo 113-8421, Japan

[4]Department of Neurodegenerative and Demented Disorders, Juntendo University Graduate School of Medicine, Tokyo, Japan.

[5]Institute for Molecular and Cellular Regulation, Gunma University, Maebashi, Japan.

[*]Author for correspondence (Tel: +81-42-676-5419; E-mail: tagaya@toyaku.ac.jp or karasaki@toyaku.ac.jp)

KEY WORDS: Autophagy, Evolution, Lipid droplet, Mitochondrial fission, Syntaxin 17

Summary Statement

Stx17 is an ancient SNARE paralog, but has been lost in multiple lineages. Because of diverse structures in the C-terminal tail, Stx17 plays different roles in different organisms.

ABSTRACT

Mammalian syntaxin 17 (Stx17) has several functions, other than membrane fusion, including mitochondrial division, autophagosome formation and lipid droplet expansion. Different from conventional syntaxins, Stx17 has a long C-terminal hydrophobic region with a hairpin-like structure flanked by a basic amino acid-enriched C-terminal tail. Although Stx17 is one of the six ancient SNAREs and present in diverse eukaryotic organisms, it has been lost in multiple lineages during evolution. In the present study, we compared the localization and function of fly and nematode Stx17s expressed in HeLa cells with those of human Stx17. We found that fly Stx17 predominantly localizes to the cytosol and mediates autophagy, but not mitochondrial division. Nematode Stx17, on the other hand, is predominantly present in mitochondria and facilitates mitochondrial division, but is irrelevant to autophagy. These differences are likely due to different structures in the C-terminal tail. Non-participation of fly Stx17 and nematode Stx17 in mitochondrial division and autophagy, respectively, was demonstrated in individual organisms. Our results provide an insight into the evolution of Stx17 in metazoa.

INTRODUCTION

The syntaxin family of proteins is one of the families of the soluble NSF attachment protein receptors (SNAREs) and participates as a target/Qa-SNARE in membrane fusion in eukaryotic cells (Jahn and Scheller, 2006). Syntaxins are tail-anchored proteins and possess a

homologous coiled-coil domain of 60-70 amino acids responsible for membrane fusion, termed the SNARE motif, which is flanked by a C-terminal transmembrane domain consisting of 17-24 hydrophobic amino acids, in some cases, followed by a short C-terminal tail (Jahn and Scheller, 2006).

Syntaxin 17 (Stx17) is one of the six ancient eukaryotic Qa-SNAREs, but has been lost in multiple lineages including yeast during evolution (Arasaki et al., 2015). It is unique in that it has a long C-terminal hydrophobic domain (CHD) consisting of 44 amino acids divided by Lys254, followed by a C-terminal tail (Arasaki et al., 2015). Although the CHD of Stx17 is well conserved, the structure of the C-terminal tail varies among organisms. Mammalian and nematode Stx17 possess several positively charged amino acids, whereas the C-terminus of fly Stx17 is enriched in negatively charged residues (Fig. 1A).

Stx17 was originally discovered as a SNARE that is abundantly expressed in steroidogenic cells and regulates the smooth endoplasmic reticulum membrane dynamics (Steegmaier et al., 2000). However, later studies demonstrated that it has several functions including those unrelated to membrane fusion (Tagaya and Arasaki, 2017). Mizushima and colleagues showed that mammalian Stx17 translocates likely from the cytosol to autophagosomes and participates in the fusion between autophagosomes and endo/lysosomes in coordination with SNAP29 and VAMP8 (Itakura et al., 2012; Tsuboyama et al., 2016). Recruitment of Stx17 to autophagosomes is probably assisted by LC3 and immunity-related GTPase M (IRGM) (Kumar et al., 2018). The role of Stx17 in autophagosome fusion with endo/lysosomes is conserved in *Drosophila* (Takáts et al., 2013), but yeast has no Stx17 ortholog (Arasaki et al., 2015). This is surprising given that autophagy is an evolutionally conserved mechanism to protect eukaryotic cells from starvation and other stresses. Yoshimori and colleagues demonstrated that Stx17 participates in autophagosome formation at the mitochondria-associated membrane (MAM), where it

recruits the Vps34-containing class III phosphatidylinositol 3-kinase complex through interaction with a subunit of the kinase complex, Atg14L (Hamasaki et al., 2013). The implication of Stx17 in autophagosome formation is somewhat contradictory to the results of Mizushima and colleagues, but recent results from several laboratories including us confirmed the involvement of Stx17 in the early stage of autophagy (Arasaki et al., 2015, 2017; Kumar et al., 2019; Machihara and Namba, 2019, Xian et al., 2019). We have demonstrated that in fed cells Stx17 localizes to the MAM and mitochondria and facilitates mitochondrial division by preventing Rab32-PKA-mediated phosphorylation of Drp1 (Arasaki et al., 2015) and promoting dephosphorylation of Drp1 by the mitochondrial protein phosphatase PGAM5 (Sugo et al., 2018). The microtubule-associated protein MAP1B-LC1 is responsible for the link of Stx17 with Drp1 and microtubules (Arasaki et al., 2018). Upon starvation, MAP1B-LC1 at Thr217 is dephosphorylated by unknown protein phosphatase(s), inducing Stx17 to dissociate from MAP1B-LC1 and associate with Atg14L (Arasaki et al., 2018). Under energy excess conditions, i.e., in the presence of oleic acid, Stx17 interacts with ACSL3, an enzyme responsible for acyl-CoA formation, and supports lipid droplet expansion (Kimura et al., 2018, 2019). It seems that Stx17 utilizes different sites for the interaction with its various partners: it interacts with Atg14L, LC3 and ACSL3 principally through the SNARE motif, with PGAM5 through the CHD and with Drp1 through the C-terminal tail (Arasaki et al., 2015; Diao et al., 2015; Kimura et al., 2018; Kumar et al., 2018; Sugo et al., 2018).

In addition to the controversy regarding which stage of autophagy Stx17 participates in, the localization of Stx17 has also been disputed. Mizushima and colleagues showed that a significant fraction of Stx17 is present in the cytosol and translocates from the cytosol to autophagosomes, but not isolation membranes (Itakura et al., 2012; Tsuboyama et al., 2016).

Yoshimori' s group and our laboratory found that Stx17 is almost exclusively associated with membranes (Arasaki et al., 2015; Hamasaki et al., 2013).

In the present study, we expressed fly and nematode Stx17s in HeLa cells and examined, in comparison with mammalian Stx17, their localization and role in mitochondrial division, autophagy and lipid droplet formation. We found that fly and nematode Stx17, when expressed in mammalian cells, principally localize to the cytosol and mitochondria, respectively. Moreover, in contrast to the fact that mammalian Stx17 can regulate both mitochondrial division and autophagy, fly and nematode Stx17 only mediate autophagy and mitochondrial division, respectively. All Stx17 species can interact with ACSL3 and promotes lipid droplet expansion. These results suggest that in certain organisms Stx17 lost some functions during evolution.

RESULTS

Endogenous Stx17 exclusively associates with membranes

Given the controversy regarding the localization of mammalian Stx17, we first examined whether Stx17 is present in the cytosol in a variety of human cell lines. We used, in addition to HeLa cells (derived from epidermoid), THP-1 (monocyte), HEK293T (embryonic kidney), Huh7 (liver) and MDA-MB-231 (mammary grand). In all the cell lines examined, Stx17 was found to be almost exclusively associated with membranes (Fig. 1B).

Localization of fly and nematode Stx17s expressed in HeLa cells

We next examined the localization of FLAG-tagged human, fly, and nematode Stx17s expressed in HeLa cells by immunofluorescence (IF) microscopy and subcellular fractionation. As reported previously (Arasaki et al., 2015), human Stx17 (hStx17) exhibited

a mitochondria-like pattern at the level of microcopy (Fig. 1C, top row), and subcellular fractionation showed its presence in the microsome, MAM, and mitochondria (Fig. 1D, top left), as seen in endogenous Stx17 (Arasaki et al., 2015). On the other hand, expressed FLAG-tagged *Drosophila melanogaster* Stx17 (dStx17) was found to be predominantly present in the cytosol (Fig. 1C, middle row), whereas FLAG-tagged *Caenorhabditis elegans* Stx17 (cStx17) was present in mitochondria with some in the cytosol (Fig. 1C, bottom row). These distributions were confirmed by subcellular fractionation (Fig. 1D, top right and bottom left).

When HeLa cells were subjected to starvation, hStx17 and dStx17 were found to form puncta positive for the autophagosomal marker LC3, whereas cStx17 was not (Fig. 1E, top images and bottom right graph). In subcellular fractionation experiments, dStx17 was found in the microsome fraction, as well as the cytosolic fraction, in starved cells (Fig. 1E, bottom left panel), in contrast to cells grown under normal conditions (Fig. 1D, top right panel). These results unequivocally showed that expressed Stx17s from different organisms localize differently in HeLa cells.

The C-terminal tail is a determinant for localization

The amino acid sequence of Stx17, in particular the sequence of the CHD, is conserved in metazoa, but the C-terminal tail varies among organisms (Fig. 1A). To determine whether the C-terminal tail is responsible for the localization of Stx17s, we removed the C-terminal tail and examined their localization. The mitochondrial-like distribution appeared to be changed to cytosolic distribution upon removal of the C-terminal tail from hStx17 and cStx17 (Fig. 2A, top and bottom rows). Consistently, most hStx17ΔC-tail and cStx17ΔC-tail were recovered in the cytosol fraction on fractionation analysis (Fig. 2B, left and right).

Interestingly, dStx17ΔC-tail showed a punctate pattern (Fig. 2A, middle row), and a substantial fraction was recovered in the membrane fraction (Fig. 2B, middle). These results suggest that the C-terminal tail of Stx17s is a determinant for localization and that fly C-tail prevents the association of dStx17 with membranes under nutrient-rich conditions. When the C-terminal tail was removed, the resultant hStx17ΔC-tail was not redistributed to autophagosomes, whereas dStx17ΔC-tail was targeted to autophagosomes upon starvation (Fig. 2C).

To confirm that the C-terminal tail of Stx17s is a determinant for localization, we constructed chimera between different species (Fig. S1A,D,G). When the C-terminal tail of hStx17 was replaced with that of dStx17 (designated as hStx17d), the mitochondria-like distribution was disrupted (Fig. S1B, middle row), whereas the mitochondria-like pattern was not changed when the C-terminal tail of hStx17 was replaced with that of cStx17 (hStx17c) (bottom row). The cytosolic localization of hStx17d and the membrane-bound localization of hStx17c were confirmed by centrifugation analysis (Fig. S1C, middle and right). On the other hand, when the C-terminal tail of dStx17 was replaced with that of hStx17 (dStx17h) or cStx17 (dStx17c), the resultant chimeras exhibited mitochondria-like localization (Fig. S1E, middle and bottom rows). The membrane association of dStx17h and dStx17c was confirmed by centrifugation analysis (Fig. S1F, middle and right). Replacement of the C-terminal tail of cStx17 with that of hStx17 (cStx17h) did not give a significant effect on the mitochondria-like localization (Fig. S1H, middle row, and Fig. S1I, middle), whereas replacement of the C-terminal tail of cStx17 with that of dStx17 (cStx17d) caused the resultant chimera to be present in the cytosol (Fig. S1H, bottom row, and Fig. S1I, right).

Because both human and nematode Stx17 proteins have basic residues at the C-terminal tail (Fig. 1A), we reasoned that these positive charges determine MAM/mitochondria localization. We therefore replaced Lys-241, Lys-244 and Arg-245 of nematode Stx17 with

Ala (cStx17KKRA). The resultant mutant exhibited cytosolic localization (Fig. 2D), suggesting that positive charges at C-terminal tail are critical for membrane association and MAM/mitochondria targeting.

We previously demonstrated that Lys-254 in hStx17 is critical for targeting to autophagosomes as well as MAMs (Arasaki et al., 2015). Consistently, the replacement of Lys-248 in dStx17, corresponding to Lys-254 in hStx17 (Fig. 1A), with Ala (dStx17K248A) abrogated the attachment of the resultant mutant to autophagosomes under starvation conditions (Fig. 2E, top row). When Ala-222 in cStx17, corresponding to the position of Lys-254 in hStx17, was replaced to Lys, the resultant mutant failed to target to autophagosomes (Fig. 2E, bottom row), suggesting that Lys-254 is required, but not enough for targeting to autophagosomes.

cStx17, but not dStx17, can promote mitochondrial fission by interacting with Drp1 in HeLa cells

It has been reported that mammalian syntaxin can function in yeast (Nakamura et al., 2000). We therefore tested whether dStx17 and cStx17 can compensate for the loss of endogenous Stx17 from HeLa cells. To this end, endogenous Stx17 in HeLa cells was knocked down by siRNA used in previous studies (Arasaki et al., 2015, 2017, 2018) and a plasmid encoding hStx17, dStx17 or cStx17 was transfected.

We first examined mitochondrial length. As reported previously (Arasaki et al., 2015), Stx17 depletion (Fig. 3A, bottom left) caused mitochondrial elongation (top left) and hStx17 can rescue this phenotype (right, top row). Expression of cStx17 (Fig. 3A, right, bottom row), but not dStx17 (right, middle row), can compensate for the loss of endogenous Stx17. The quantitative data confirmed this notion (Fig. 3B). As Stx17 promotes mitochondrial fission by preventing Drp1 from PKA-mediated inactivation (Arasaki et al., 2015) and by

supporting Drp1 activation via protein phosphatase PGAM5 (Sugo et al., 2018), we examined whether cStx17 can interact with endogenous Drp1 in HeLa cells using proximity ligation assay (PLA). As expected, cStx17, as well as hStx17, gave positive signals, whereas a very low signal was detected for dStx17 (Fig. 3C,D). Immunoprecipitation experiments demonstrated the interaction of Drp1 K38A, a Drp1 mutant that is defective in GTP hydrolysis but retains some GTP-binding ability (Smirnova et al., 1998), and thereby exhibits an enhanced binding to Stx17 compared to wild-type Drp1 (Arasaki et al., 2015), with hStx17 and cStx17, but much less with dStx17 (Fig. 3E).

dStx17, but not cStx17, can promote autophagosome formation by interacting with Atg14L in HeLa cells

Next, we examined whether dStx17 and cStx17 can rescue an autophagosome formation defect due to endogenous Stx17 depletion from HeLa cells. Consistent with our and other reports (Arasaki et al., 2015, 2017; Kumar et al., 2019, Machihara and Namba, 2019; Xian et al., 2019), endogenous Stx17 knockdown blocked autophagosome formation (Fig. 4A, left, bottom row). This phenotype was found to be rescued by the expression of dStx17 (Fig. 4A, right, middle row), but not cStx17 (right, bottom row). The numbers of autophagosomes formed were comparable between cells expressing hStx17 and dStx17 (Fig. 4B).

As hStx17 changes its binding partner from Drp1 to Atg14L upon starvation (Arasaki et al., 2015; Hamasaki et al., 2013), we examined whether dStx17, but not cStx17, interacts with Atg14L under starved conditions. As expected, dStx17, but not cStx17, showed proximity to endogenous Atg14L in HeLa cells (Fig. 4C, D). Immunoprecipitation experiments confirmed the interaction of Atg14L with hStx17 and dStx17, but not with cStx17 (Fig. 4E).

Both dStx17 and cStx17 can mediate lipid droplet expansion in HeLa cells

Our recent studies demonstrated that hStx17 promotes lipid droplet expansion by interacting with acyl-CoA synthase long chain family member 3 (ACSL3) (Kimura et al., 2018, 2019). In contrast to the cases of mitochondrial division and autophagosome formation, both dStx17 and cStx17 could compensate for the loss of endogenous Stx17 in terms of lipid droplet expansion (Fig. 5A,B). In addition, both proteins as well as hStx17 could interact with ACSL3 (Fig. 5C,D). The interaction of all Stx17 species with ACSL3, but not ACSL3ΔGATE, a mutant lacking a Stx17-interacting domain (Kimura et al., 2018), was confirmed by immunoprecipitation experiments (Fig. 5E).

To test the specificity of the interaction of dStx17 and cStx17 with human ACSL3, we examined whether these proteins can interact with ACSL1 because hStx17 cannot interact with ACSL1 (Kimura et al., 2018). Compared with ACSL3, much lower signals were detected between ACSL1 and dStx17 and cStx17 as well as hStx17 (Fig. 5D). On the other hand, moderate signals were detected between ACSL4 and all Stx17 species. These results emphasize the specificity of the ACSL3-Stx17 interaction and suggest that this interaction is conserved across the species of organisms.

Role of Stx17 in *Drosophila* and C. *elegans*

To exclude the possibility that the predicted roles of Stx17 in *Drosophila* and C. *elegans* from the results obtained using HeLa cells are artifacts due to heterologous expression of Stx17 in human cells, we explore the roles of Stx17 in fly and nematode using *Drosophila* Schneider 2 (S2) cells and living organisms.

Consistent with the data obtained using HeLa cells, endogenous dStx17 was found to be mainly present in the cytosol of S2 cells, whereas a considerable fraction of dStx17 was observed in the membrane fraction in starved cells (Fig. 6A). A similar result was obtained for FLAG-tagged dStx17 expressed in S2 cells (Fig. 6B). A low molecular weight dStx17 species, marked by asterisk in Fig. 6A, was found to be associated with membranes without starvation treatment (Fig. 6A). This may be a C-terminally cleaved form of dStx17, as a C-terminally truncated dStx17 was found to be associated with membranes in HeLa cells (Fig. 2B). Alternatively, the low molecular weight band may be a nonspecific band. The localization of hStx17 and cStx17 in S2 cells were essentially the same as that observed in HeLa cells: both were found to be associated with membranes regardless of nutrient situation (Fig. 6B).

We next examined whether Stx17 participates in mitochondrial division in *Drosophila*. A previous study showed that, when mitochondrial division is attenuated by knockdown of Drp1 or Mff in S2 cells, mitochondrial clustering occurs at the perinuclear region perhaps due to mitochondrial elongation (Gandre-Babbe and van der Bliek, 2008). We therefore knocked down Stx17 in S2 cells (Fig. 6C) and examined mitochondrial morphology. No mitochondrial clustering was observed in Stx17-depleted cells, although slight vacuolation may have occurred (Fig. 6D). The latter may be a consequence of autophagy inhibition due to loss of dStx17. Next, we knocked out Stx17 in *Drosophila* and examined mitochondrial morphology. As shown in Fig. 6E, no significant difference in the length of flight muscle mitochondria was observed between wild-type and Stx17-ablated *Drosophila,* although the cristae integrity was somewhat affected, showing the areas where the electron density was losing. Overall, these results are consistent with the data obtained from heterologous expression of dStx17 in HeLa cells.

Next, we explored the role of Stx17 in *C. elegans*. To this end, we examined allophagy, fertilization-triggered autophagy to remove sperm mitochondria (Sato and Sato, 2011, 2012). In one-cell stage embryos, paternal mitochondria were observed in both wild-type and *C. elegans* mutants lacking Stx17 (*syx17*) (Fig. 7A, 1-cell). In the 8-16 cell stage, paternal mitochondria were lost due to allophagy not only in wild-type but also the two *syx17* mutants (Fig. 7A, 8-16 cell), suggesting that allophagy occurs in the absence of Stx17. This is consistent with the observation that cStx17 cannot compensate for the defect in autophagy due to the loss of hStx17 in HeLa cells.

hStx17 cannot compensate for dStx17 deletion in *Drosophila*

We next examined whether hStx17 and cStx17 can function in *Drosophila*. To this end, we expressed hStx17 and cStx17 in *Drosophila* depleted of endogenous Stx17 ($syx17^{-/-}$) and examined the emergence rate. Although expression of dStx17 partially restored the emergence rate, no recovery was observed upon expression of hStx17 or cStx17 (Fig. S2A). Expression of hStx17 or cStx17 appeared to rather deteriorate the emergence efficiency. Ablation of dStx17 caused a loss of LysoTracker staining, perhaps due to a defect in autophagy. Expression of dStx17 recovered LysoTracker staining, whereas expression of hStx17 or cStx17 failed to recover the staining (Fig. S2B). Given that hStx17 and cStx17, unlike dStx17, stably associate with membranes (Fig. 1D), it is tempting to speculate that the property of stable membrane association of Stx17 is toxic for *Drosophila* cells.

DISCUSSION

Although Stx17 is an ancient eukaryotic Qa-SNARE, it has been lost in multiple lineages during evolution (Arasaki et al., 2015). This is rather surprising because it plays an important role in autophagy, a conserved mechanism in eukaryotic cells (Mizushima et al., 2011). To

gain insight into the relationship between function and evolution of Stx17, we expressed Stx17s derived from fly and nematode in HeLa cells and examined their localization and function. Our results demonstrated that the localization of Stx17 is species-specific: hStx17 is present in the ER, MAM and mitochondria, whereas dStx17 predominantly localizes to the cytosol. cStx17, like hStx17, is principally associated with membranes, but its localization seems to be limited to mitochondria. Our deletion and chimera construction analyses showed that the C-tail of Stx17 is a determinant for membrane association: Stx17s with positively charged C-tail (hStx17 and cStx17) localize to the MAM and mitochondria, whereas Stx17 with negatively charged C-terminal (dStx17) is principally present in the cytosol. It should be noted that the major determinant for membrane association is likely the CHD. Even dStx17, the CHD could associate with membranes upon removal of the acidic C-tail. Therefore, the C-tail of Stx17 plays a role in fine-tuning the localization of Stx17.

We could infer that the ancient SNARE Stx17 had multifunctional roles (mitochondrial division, autophagosome formation and lipid droplet biogenesis), in addition to membrane fusion, and became not essential at a certain stage in the evolution of eukaryotic cells. This may be accomplished during evolution by the emergence of syntaxin paralogs that have redundant function with Stx17. Therefore, Stx17 has been lost in multiple lineages, including yeast. The reason why Stx17 is not conserved in yeast is probably due to the presence of a different set of SNAREs involved in autophagy. In yeast, Ykt6, Vam3, Vti1 and Vam7 participate in autophagosome-vacuole fusion (Bas et al., 2018; Gao et al., 2018, Kriegenburg et al., 2019). A recent study revealed that in mammals Ykt6 also functions as a SNARE for autophagosome-endo/lysosome fusion (Matsui et al., 2018). Emergence of other scaffold proteins or evolution of proteins involved in mitochondrial division and autophagosome formation might have diminished the requirement of Stx17. As a consequence, Stx17s in

nematode and fly lost the ability for autophagosome formation and mitochondrial division, respectively.

Another important finding in this study is that Stx17 is almost exclusively associated with membranes in mammalian cells. Given its presence in the cytosol, Mizushima and colleagues proposed that Stx17 translocates to autophagosomal membranes from the cytosol during autophagosome formation. In their data, a significant fraction of Stx17 was present in the cytosol (Itakura et al., 2012). Although the reason of this discrepancy is not clear at present, one possible explanation is that they examined the localization of expressed, not endogenous, Stx17. Overexpression may cause a partial detachment of Stx17 in certain cells. Alternatively, under certain conditions, Stx17 may detach from membranes and stably stay in the cytosol. We favor the idea that Stx17 is stationary associated with the MAM and mitochondria, and upon autophagosome formation it translocates from the MAM to autophagosomes. As discussed in our previous report (Sugo et al., 2018), the energy barrier for the translocation of membrane proteins between closely apposed membranes, i.e., at membrane contact sites, may be low, and some proteins could shuttle between the organelles. Indeed, it was reported that certain proteins such as FKBP38 and Bcl-2 can translocate from mitochondria to the ER during mitophagy (Saita et al., 2013). Another example is the translocation of cytochrome b5 from mitochondria to autophagosomes, perhaps through the MAM (Hailey et al., 2010). For this transfer, the hairpin-like membrane-anchor of cytochrome b5 is essential. Stx17 also possesses such a structure, but perhaps the anchor is more shallowly embedded in membranes so that Lys254 faces the cytosol. Although this structure is similar to those of proteins targeting to lipid droplets (Kory et al., 2016), we have never seen that Stx17 localizes to lipid droplets (Kimura et al., 2018, 2019). This is perhaps due to the glycine-zipper-like structure of the CHD (Itakura et al., 2012).

dStx17 and cStx17 can compensate for the loss of hStx17 function with regard to lipid droplet formation. Consistently, both Stx17s as well as hStx17 interact with ACSL3, the enzyme responsible for lipid droplet biogenesis among ACSL family members (Kassan et al., 2013; Kimura et al., 2018). Although our previous results showed that hStx17 interacts with ACSL3, but not with other ACSL family members including ACSL4 (Kimura et al., 2018), we detected a positive signal between Stx17 and ACSL4. This may be partly due to the effect of overexpression of Stx17. In HeLa cells, the expression level of Stx17 may be low, and therefore the proximity between the endogenous ACSL4 and Stx17 may not be detectable. The present observation that Stx17 from different species can interact with ACSL3 is consistent with the fact that the SNARE motif of hStx17 is required for the interaction with ACSL3 and lipid droplet formation (Kimura et al., 2018). The SNARE motif is relatively well conserved in human, fly and nematode Stx17s (Fig. 1A).

In conclusion, our results shed light on the correlation between the diverse structure of the C-terminal tail and multiple functions of Stx17. Unfortunately, we could not determine whether Stx17 in *C. elegans* plays a role in mitochondrial division, although cStx17 was found to compensate for the defect in mitochondrial division due to loss of Stx17 in HeLa cells. This question should be addressed in future work.

MATERIALS and METHODS

Antibodies

The following antibodies were obtained from Sigma-Aldrich: Human calnexin (CNX) (No. 610523: 1/1000 for IB), monoclonal FLAG (No. F3165: 1/300 for IF and PLA), polyclonal FLAG (No. F7425: 1/3000 for IB, 1/300 for IF and PLA) and monoclonal α-tubulin (No. T6074: 1/3000 for IB). The following antibodies were obtained from BD Bioscience

Pharmingen: Drp1 (No. 611112: 1/40 for PLA) and Tom20 (No. 612278: 1/300 for IF, 1/1000 for IB). The following antibodies were obtained from Abcam: ACSL1 (No. ab76702: 1/100 for PLA) and polyclonal α-tubulin (No. ab15246: 1/3000 for IB). An anti-LC3 antibody (No. PM036: 1/150 for IF) was purchased from MBL. An anti-Atg14L antibody was purchased from Proteintec (No. 24412-1-AP: 1/200 for PLA). Alexa Fluor® 488 and 594 goat anti-mouse and -rabbit antibodies (No. A-11001, A-11005, A-11008 and A-11012: 1/200 for IF) were obtained from Thermo Fisher Scientific. Antibodies against ACSL3 and ACSL4 were obtained from GeneTex (No. GTX112431, 1/100 for PLA) and Santa Cruz Biotechnology (No. sc-134507, 1/100 for PLA), respectively. An anti-*Drosophila* CNX was purchased from DSHB (No. Cnx99A 6-2-1, 1:10 for IF, 1/1000 for IB). A guinea pig anti-Stx17 antibody (1/5000 for IB) was kindly supplied by Dr. G. Juhász at Eotvos Lorand University, Hungary. The preparation of a polyclonal antibody against Stx17 was described previously (Arasaki et al., 2015). Goat anti-mouse IgG (H + L)-HRP conjugate (No.1706516, 1/3000 for IB) and goat anti-rabbit IgG (H+L)-HRP conjugate (No.1706515, 1/3000 for IB) were obtained from Bio-Rad Goat anti-guinea pig IgG (H+L)-HRP conjugate (No. 106-035-003, 1/3000 for IB) was obtained from Jackson ImmunoResearch Laboratories.

Plasmids

Preparation of FLAG-tagged human Stx17 constructs was described previously (Arasaki et al., 2015). cDNA encoding fly Stx17 was kindly supplied by Dr. G. Juhász. cDNA encoding nematode Stx17 was purchased from Open Biosystems. Each cDNA for Stx17 was subcloned into the EcoRI/BamHI site of pFLAG-CMV-6c. Using these plasmids, plasmids encoding the C-terminal tail were constructed by inverse PCR. To the plasmids, Stx17 fragments depleted of the C-terminal tail were amplified and inserted so as to obtain chimera constructs. FLAG-hStx17 mutant (ΔC-tail), FLAG-dStx17 mutants (ΔC-tail, K248A) and

FLAG-cStx17 mutants (ΔC-tail, KKRA and A222K) were generated by inverse PCR. The plasmid for pUAST FLAG-hStx17, FLAG-dStx17 and FLAG-cStx17 were constructed by inserting the cDNAs for FLAG-hStx17, FLAG-dStx17 and FLAG-cStx17 into the EcoRV site of the pUAST vector. Construction of other plasmids was described previously (Arasaki et al., 2015; Kimura et al., 2018).

Cell culture

293T and Huh7 cells were grown in DMEM supplemented with 50 IU/ml penicillin, 50 μg/ml streptomycin and 10% fetal calf serum. MDA-MB-231 cells were grown in 50% DMEM and 50% RPMI 1640 supplemented with the same materials. HeLa cells (RIKEN, RCB0007) were cultured in α-MEM supplemented with the same materials plus 2 mM L-glutamine. For starvation of cells, the cells were rinsed with PBS twice and then incubated in Earle's balanced salt solution (EBSS). S2 cells were grown in Schneider's *Drosophila* Medium supplemented with 50 IU/ml penicillin, 50 μg/ml streptomycin and 10% fetal calf serum. For starvation S2 cells were rinsed with PBS twice, and then incubated in PBS containing 2 mg/ml glucose.

Subcellular fractionation

Subcellular fractionation was performed as described previously (Arasaki et al., 2015). Experiments were repeated three times with similar results. To separate the cytosol and total membrane fractions, cell lysates were centrifuged for 20 min at 98,000 x g.

Transfection

Transfection of mammalian cells was carried out using polyethylenimine (Polysciences) or LipofectAMINE 2000 (Thermo Fisher Scientific). Transfection of S2 cells was carried out using TransIT Insect Transfection Reagent (Mirus Bio). Usually, 1 μg of plasmid was used for transfection of cells cultured on 6 well plates. However, because of low expression efficiency, 2 μg of plasmid was used for the expression of cStx17 in mammalian cells. To express proteins in S2 cells, pAct5C-Gal4 and pUAST plasmids were co-transfected.

RNA interference

The sequence of siRNA targeting the 3'-UTR of human Stx17 is 5'-GGAAAUUAAUGAUGUAAGA-3'. This siRNA effectively knocked down endogenous Stx17 in HeLa cells (Arasaki et al., 2015). The sequence of siRNA targeting *Drosophila* Stx17 is 5'- CAACUCAAUUUCCAGCUGGAG -3'. The siRNAs were purchased from Japan Bio Services (Asaka, Japan). Cells were grown on 6 well plates, and siRNA was transfected at a final concentration of 200 nM using Oligofectamine (Thermo Fisher Scientific) for mammalian cells and Lipofectamine RNAiMAX (Thermo Fisher Scientific) for S2 cells according to the manufacturers' protocols.

Immunoprecipitation

293T cells expressing FLAG-tagged proteins were lysed in lysis buffer (20 mM Hepes-KOH (pH 7.2), 150 mM KCl, 2 mM EDTA or 2 mM $MgCl_2$, 1 mM dithiothreitol, 1 μg/ml leupeptin, 1 μM pepstatin A, 2 μg/ml aprotinin and 1 mM phenylmethylsulfonyl fluoride) containing 1% Triton X-100 or 0.1% digitonin. After centrifugation, the supernatants were

immunoprecipitated with anti-FLAG M2 affinity beads (Sigma-Aldrich). The bound proteins were eluted with SDS sample buffer and then analyzed by IB.

IF microscopy

For IF microscopy, HeLa and S2 cells were fixed for 20 min with 4% paraformaldehyde at room temperature or with ice-cold methanol, mounted with mounting medium (Dako) or SlowFade™ Diamond Antifade Mountant with DAPI (Thermo Fisher Scientific), and then observed under an Olympus Fluoview 1000 or 1200 laser scanning microscope. To stain mitochondria in S2 cells, cells were incubated with 500 nM MitoTracker Red CMXRos (Thermo Fisher Scientific) for 5 min at 25°C. Representative images of at least three independent experiments are shown in figures.

Quantification of LC3-positive and other autophagy-related structures

The number of LC3-positive puncta and other autophagy-related structures was counted using the ImageJ software (NIH).

Mitochondria length

The length of mitochondria was measured as described previously (Arasaki et al., 2015).

PLA

PLA was conducted using a PLA kit (Sigma-Aldrich) according to the manufacturer's protocol. Determination of the number of PLA dots was performed using the ImageJ software (NIH). In each experiment, 30 cells were examined. To identify cells expressing

FLAG-tagged proteins, a plasmid for GFP (0.2 μg) was co-transfected with FLAG-tagged constructs (1 μg). GFP-expressing cells were deemed to express FLAG-proteins. The specificity of antibodies used for PLA was confirmed by reduction in IF signal in cells depleted of antigens and in PLA signal in cells without expression of FLAG-tagged Stx17 (data not shown).

Drosophila genetics and histochemistry

Fly cultures and crosses were performed on standard fly food containing yeast, cornmeal, molasses and 20 mg/mL sucrose, and the flies were raised at 25°C. *Act5C-Gal4*, *UAS-LacZ* and $Syx17^{LL06330}$ (Kyoto stock number 140948) lines were obtained from the Bloomington *Drosophila* Stock Center or the Kyoto Stock Center.

The 3rd instar larvae were starved in the 20% sucrose/HL-3 (pH 7.2) solution for 3 h. Larvae were dissected in the HL-3 solution and the fat bodies were stained with HL-3 containing 1 μM LysoTracker Red (Thermo Fisher Scientific) for 10 s. Images of the fat bodies mounted with HL-3 were taken using a laser-scanning microscope system (TCS-SP5, Leica). Transmission electron microscopy images were obtained at the Laboratory of Morphology and Image Analysis, Research Support Center, Juntendo University Graduate School of Medicine.

Worm strains and analysis

The methods for the handling and culturing of *C. elegans* were essentially the same as those described previously (Sato et al., 2018). The deletion alleles of *syx17/VF39H2L.1 (tm3181* and *tm3244)* were provided by Shohei Mitani of the Japanese National Bioresource Project for the Experimental Animal "Nematode *C. elegans*." The *tm3181* contains a 1239-bp

deletion that removes the start codon of *syx17*. In the *tm3244* mutant, a 955-bp region including the 4th exon encoding the SNARE motif is deleted. These mutants are viable and fertile at 20°C. They were outcrossed with the wild-type three times and then crossed with transgenes *dkIs399[Ppie-1::GFP::lgg-1, unc-119 (+)]* (Sato and Sato, 2011) and *dkIs698[Pspe-11::hsp-6::mCherry, unc-119(+)]*(Sato et al., 2018). Embryos were dissected, mounted on agarose pads and observed by using an Olympus FV1200 confocal microscope system equipped with a 60×, 1.35 NA UPlanSApo oil-objective lens.

Statistics

The results were averaged, expressed as the mean with s.e.m. and analyzed by means of a paired Student's *t*-test followed by a Bonferroni *post hoc* test. The *p* values are indicated by asterisks in the figures with the following notations: *, $p < 0.05$, **, $p < 0.01$; ***, $p < 0.001$, n.s., not significant.

Acknowledgments

We appreciate Dr. G. Juhász at Eotvos Lorand University, Hungary, for generous gifts of an anti-*Drosophila* Stx17 antibody and a plasmid encoding *Drosophila* Stx17, Dr. S. Mitani at Tokyo Women's Medical University for providing *C. elegans* mutants, and Dr. Joel B. Dacks at University of Alberta, Canada, for his comments on this manuscript. We thank Dr. Hideshi Inoue at Tokyo University of Pharmacy and Life Sciences for his support for obtaining a cStx17 clone and Mr. Yuki Ebi for his technical assistance. We are indebted to the Laboratory of Morphology and Image Analysis, Research Support Center, Juntendo University Graduate School of Medicine for technical assistance with transmission electron microscopy analysis.

Competing interests

The authors declare no competing or financial interests.

Author contributions

This study was conceived and designed by KA and MT. SK and NT performed the experiments. YI, TI and NH performed the *Drosophila* analysis. TS and MS performed the *C. elegans* analysis. YW and HI contributed with expertise in experiments.

Funding

This work was supported in part by Grants-in-Aid for Scientific Research from JSPS KAKENHI Grant Numbers 18H02439 (to MT), 20K21531 (to YI), 19H05712 and 21H02472 (to MS), JP20J01777 (to TS) and 18H02656 and 20H05772 (to KA) and the Uehara Memorial Foundation and the Naito Foundation (to KA).

References

Arasaki, K., Mikami, Y., Shames, S. R., Inoue, H., Wakana, Y. and Tagaya, M. (2017). *Legionell*a effector Lpg1137 shuts down ER-mitochondria communication through cleavage of syntaxin 17. *Nat. Commun.* **8**, 15406.

Arasaki, K., Nagashima, H., Kurosawa, Y., Kimura, H., Nishida, N., Dohmae, N., Yamamoto, A., Yanagi, S., Wakana, Y., Inoue, H. et al. (2018). MAP1B-LC1 prevents autophagosome formation by linking syntaxin 17 to microtubules. *EMBO Rep.* **19**, e45584.

Arasaki, K., Shimizu, H., Mogari, H., Nishida, N., Hirota, N., Furuno, A., Kudo, Y., Baba, M., Baba, N., Cheng, J. et al. (2015). Role for the ancient SNARE syntaxin 17 in regulating mitochondrial division. *Dev. Cell* **32**, 304-317.

Bas, L., Papinski, D., Licheva, M., Torggler, R., Rohringer, S., Schuschnig, M. and Kraft, C. (2018). Reconstitution reveals Ykt6 as the autophagosomal SNARE in autophagosome-vacuole fusion. *J. Cell Biol.* **217**, 3656-3669.

Diao, J., Liu, R., Rong, Y., Zhao, M., Zhang, J., Lai, Y., Zhou, Q., Wilz, L. M., Li, J., Vivona, S. et al. (2015). ATG14 promotes membrane tethering and fusion of autophagosomes to endolysosomes. *Nature* **520**, 563-566.

Gandre-Babbe, S. and van der Bliek, A. M. (2008). The novel tail-anchored membrane protein Mff controls mitochondrial and peroxisomal fission in mammalian cells. *Mol. Biol. Cell* 19, 2402-2412.

Gao, J., Reggiori, F. and Ungermann, C. (2018). A novel in vitro assay reveals SNARE topology and the role of Ykt6 in autophagosome fusion with vacuoles. *J. Cell Biol.* **217**, 3670–3682.

Hailey, D. W., Rambold, A. S., Satpute-Krishnan, P., Mitra, K., Sougrat, R., Kim, P. K. and Lippincott-Schwartz, J. (2010). Mitochondria supply membranes for autophagosome biogenesis during starvation. *Cell* **141**, 656-667.

Hamasaki, M., Furuta, N., Matsuda, A., Nezu, A., Yamamoto, A., Fujita, N., Oomori, H., Noda, T., Haraguchi, T., Hiraoka, Y. et al. (2013). Autophagosomes form at ER-mitochondria contact sites. *Nature* **495**, 389-393.

Itakura, E., Kishi-Itakura, C. and Mizushima, N. (2012). The hairpin-type tail anchored SNARE syntaxin 17 targets to autophagosomes for fusion with endosomes/lysosomes. *Cell* **151**, 1256–1269.

Jahn, R. and Scheller, R. H. (2006). SNAREs—engines for membrane fusion. *Nat. Rev. Mol. Cell Biol*. **7**, 631–643.

Kassan, A., Herms, A., Fernández-Vidal, A., Bosch, M., Schieber, N. L., Reddy, B. J., Fajardo, A., Gelabert-Baldrich, M., Tebar, F., Enrich, C. et al. (2013). Acyl-CoA synthetase 3 promotes lipid droplet biogenesis in ER microdomains. *J. Cell Biol*. **203**, 985-1001.

Kimura, H., Arasaki, K., Iitsuka, M. and Tagaya, M. (2019). Syntaxin 17 recruits ACSL3 to lipid microdomains in lipid droplet biogenesis. *Contact (Thousand Oaks)* **2**, 2515256419838719.

Kimura, H., Arasaki, K., Ohsaki, Y., Fujimoto, T., Ohtomo, T., Yamada, J. and Tagaya, M. (2018). Syntaxin 17 promotes lipid droplet formation by regulating the distribution of acyl-CoA synthetase 3. *J. Lipid Res*. **59**, 805-819.

Kory, N. Farese, R. V. Jr. and Walther, T. C. (2016). Targeting Fat: Mechanisms of protein localization to lipid droplets. *Trends Cell Biol*. **26**, 535-546.

Kriegenburg, F., Bas, L., Gao, J., Ungermann, C. and Kraft, C. (2019). The multi-functional SNARE protein Ykt6 in autophagosomal fusion processes. *Cell Cycle* **18**, 639-651.

Kumar, S., Gu, Y., Abudu, Y. P., Bruun, J. A., Jain, A., Farzam, F., Mudd, M., Anonsen, J. H., Rusten, T. E., Kasof, G. et al. (2019). Phosphorylation of syntaxin 17 by TBK1 controls autophagy initiation. *Dev. Cell* **49**,130-144.

Kumar, S., Jain, A., Farzam, F., Jia, J., Gu, Y., Choi, S. W., Mudd, M. H., Claude-Taupin, A., Wester, M. J., Lidke, K. A. et al. (2018). Mechanism of Stx17 recruitment to autophagosomes via IRGM and mammalian Atg8 proteins. *J. Cell Biol*. **217**, 997-1013.

Machihara, K. and Namba, T. (2019). BAP31 inhibits cell adaptation to ER stress conditions, negatively regulating autophagy induction by interaction with STX17. *Cells* **8**, 1350.

Matsui, T., Jiang, P., Nakano, S., Sakamaki, Y., Yamamoto, H. and Mizushima, N. (2018). Autophagosomal YKT6 is required for fusion with lysosomes independently of syntaxin 17. *J. Cell Biol*. **217**, 2633-2645.

Mizushima, N., Yoshimori, T. and Ohsumi, Y. (2011). The role of Atg proteins in autophagosome formation. *Annu. Rev. Cell Dev. Biol*. **27**, 107-132.

Nakamura, N., Yamamoto, A., Wada, Y. and Futai, M. (2000). Syntaxin 7 mediates endocytic trafficking to late endosomes. *J. Biol. Chem*. **275**, 6523-6529.

Saita, S., Shirane, M. and Nakayama, K. I. (2013). Selective escape of proteins from the mitochondria during mitophagy. *Nat. Commun*. **4**, 1410.

Smirnova, E., Shurland, D. L., Ryazantsev, S. N. and van der Bliek, A. M. (1998). A human dynamin-related protein controls the distribution of mitochondria. *J. Cell Biol*. **143**, 351-358.

Sato, M. and Sato, K. (2011). Degradation of paternal mitochondria by fertilization-triggered autophagy in *C. elegans* embryos. *Science* **334**, 1141-1144.

Sato, M. and Sato, K. (2012). Maternal inheritance of mitochondrial DNA: degradation of paternal mitochondria by allogeneic organelle autophagy, allophagy. *Autophagy* **8**, 424-425.

Sato, M., **Sato, K., Tomura, K., Kosako, H. and Sato, K.** (2018). The autophagy receptor ALLO-1 and the IKKE-1 kinase control clearance of paternal mitochondria in *Caenorhabditis elegans*. *Nat. Cell Biol*. **20**, 81-91.

Steegmaier, M., Oorschot, V., Klumperman, J. and Scheller, R. H. (2000). Syntaxin 17 is abundant in steroidogenic cells and implicated in smooth endoplasmic reticulum membrane dynamics. *Mol. Biol. Cell* **11**, 2719-2731.

Sugo, M., Kimura, H., Arasaki, K., Amemiya, T., Hirota, N., Dohmae, N., Imai, Y., Inoshita, T., Shiba-Fukushima, K., Hattori, N. et al. (2018). Syntaxin 17 regulates the localization and function of PGAM5 in mitochondrial division and mitophagy. *EMBO J*. **37**, e98899.

Tagaya, M. and Arasaki, K. (2017). Regulation of mitochondrial dynamics andautophagy by the mitochondria-associated membrane. *Adv*. *Exp. Med. Biol*. **997**, 33-47.

Takáts, S., Nagy, P., Varga, Á., Pircs, K., Kárpáti, M., Varga, K., Kovács, A. L., Hegedűs, K. and Juhász, G. (2013). Autophagosomal syntaxin17-dependent lysosomal degradation maintains neuronal function in *Drosophila*. *J. Cell Biol*. **201**, 531-539.

Tsuboyama, K., Koyama-Honda, I., Sakamaki, Y., Koike, M., Morishita, H. and Mizushima, N. (2016). The ATG conjugation systems are important for degradation of the inner autophagosomal membrane. *Science* **354**, 1036-1041.

Xian, H., Yang, Q., Xiao, L., Shen, H. M. and Liou, Y. C. (2019). STX17 dynamically regulated by Fis1 induces mitophagy via hierarchical macroautophagic mechanism. *Nat. Commun.* **10**, 2059.

Figures

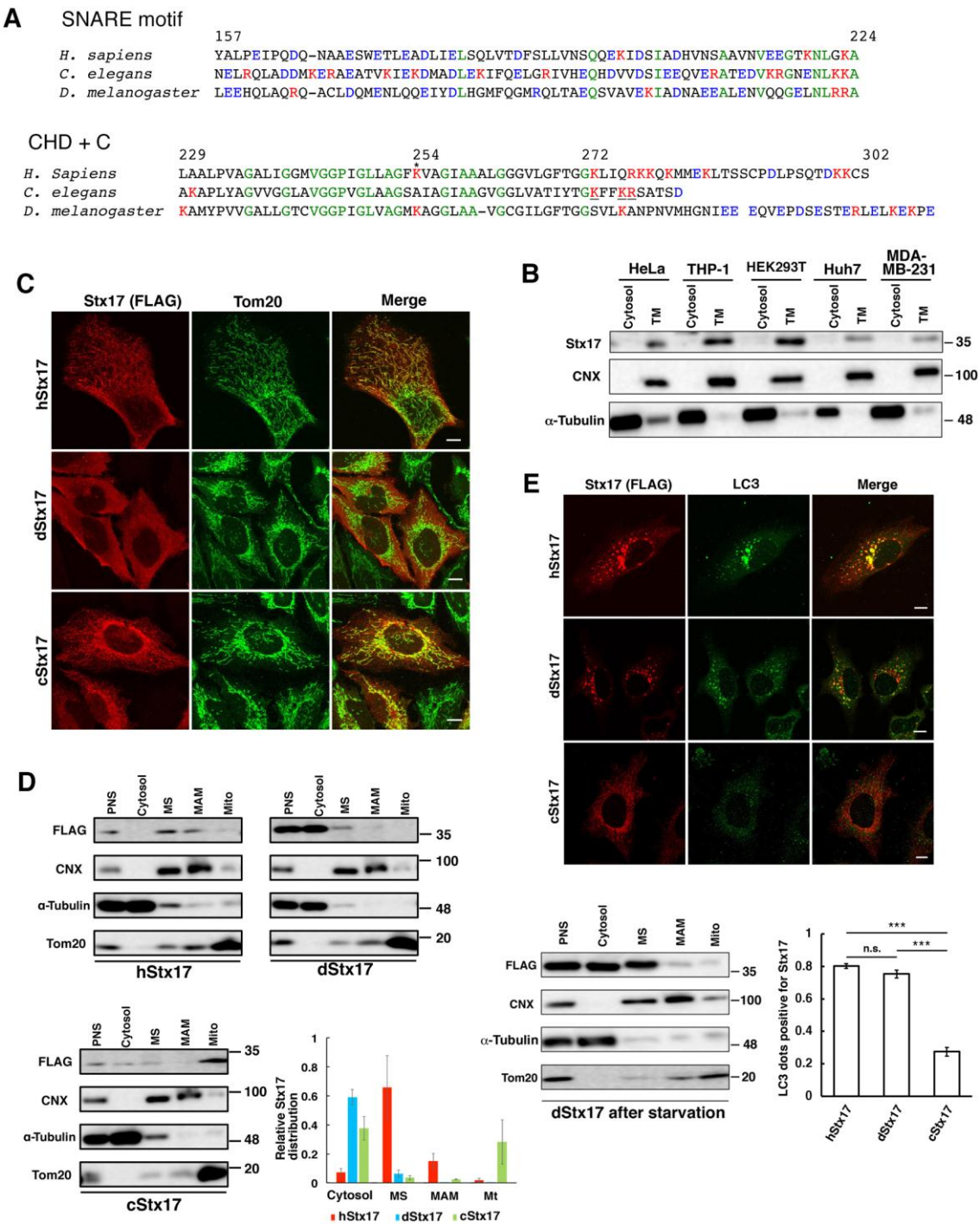

Fig. 1. Stx17s derived from different organisms localize differently in HeLa cells. (A) Comparison of the SNARE motif and C-terminal region of human, nematode and fly Stx17 species. Identical, basic and acidic amino acids are highlighted in green, red and blue, respectively. Nematode Lys-241, Lys-244 and Arg-245 are underlined, and human Lys-254 is marked by an asterisk. (B) The indicated cultured cells were lysed and centrifuged to separate the cytosol and total membrane (TM) fractions. The fractions (10 μg protein each) were analyzed by immunoblotting (IB) using the indicated antibodies. α-tubulin and CNX are markers for the cytosol and TM fractions, respectively. (C) HeLa cells were transfected with a plasmid encoding FLAG-tagged hStx17, dStx17 or cStx17. At 24 h after transfection, the cells were fixed and analyzed by IF microscopy. Scale bars, 10 μm. (D) HeLa cells expressing each Stx17 construct were lysed and subjected to subcellular fractionation, as described in Material and Methods. The fractions (8 μg protein each) were analyzed by IB using the indicated antibodies. The quantification data are shown at the bottom right. Results are mean±s.e.m. from *n*=3 independent experiments. PNS, postnuclear supernatant; MS, microsomes; Mito, mitochondria. (E) HeLa cells expressing each Stx17 construct was incubated with EBSS for 2 h, fixed and analyzed by IF microscopy (top). Scale bars, 10 μm. In the case of cells expressing dStx17, the starved cells were lysed, fractionated and analyzed IB using the indicated antibodies (bottom left). PNS, postnuclear supernatant; MS, microsomes; Mito, mitochondria. The bar graph on the bottom right shows the quantification of LC3 dots positive for FLAG-tagged Stx17 species. Results are mean±s.e.m. from *n*=3 independent experiments. In each experiment, 30 cells were examined. ***$p < 0.001$, n.s., not significant. In (B), (D) and (E), molecular size markers (kDa) are shown.

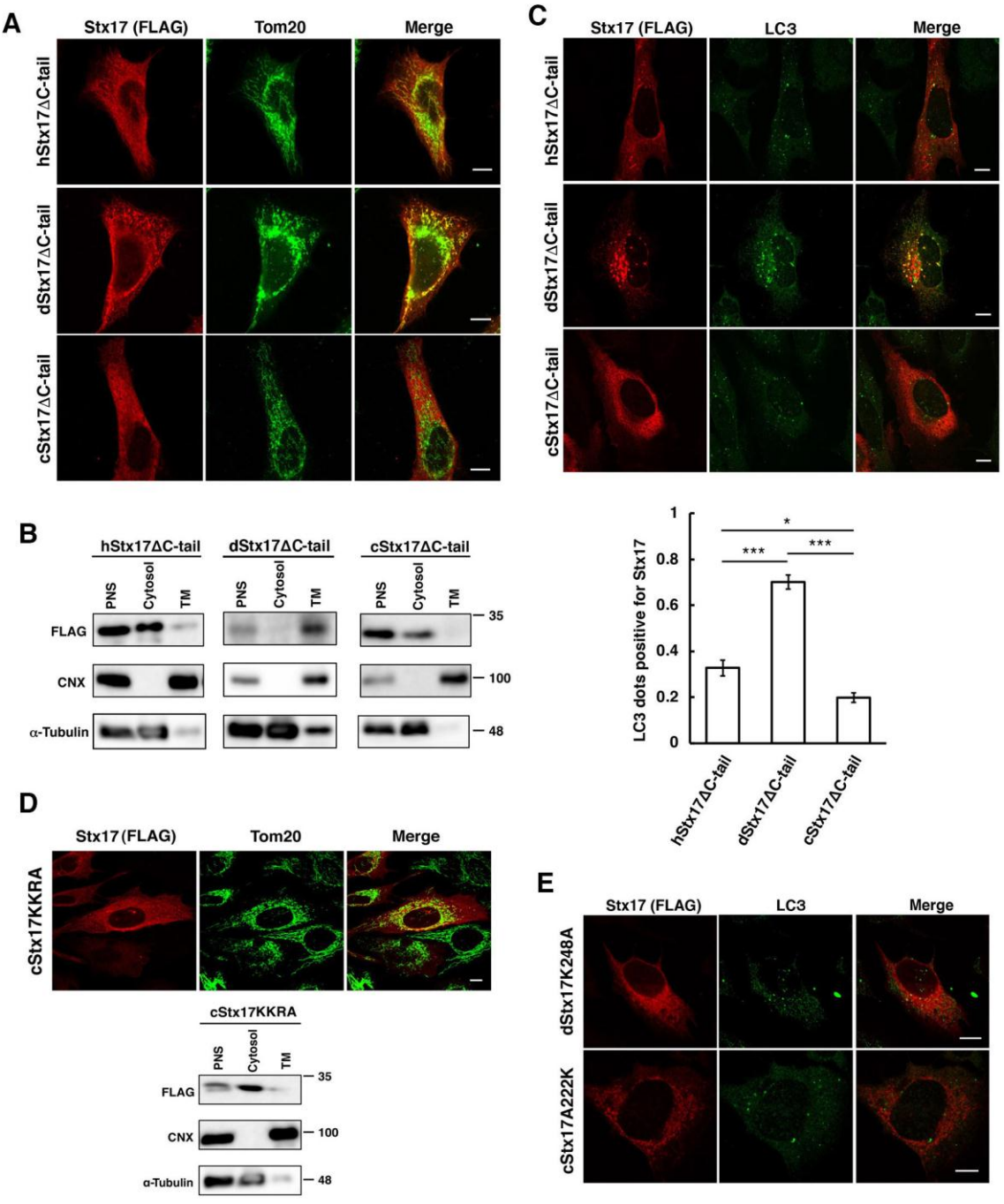

Fig. 2. The C-terminal tail of Stx17 is a determinant for localization. (A) HeLa cells were transfected with a plasmid encoding FLAG-tagged hStx17ΔC-tail, dStx17ΔC-tail or cStx17ΔC-tail. At 24 h after transfection, the cells were fixed and analyzed by IF microscopy. Scale bars, 10 μm. (B) HeLa cells expressing Stx17ΔC-tail mutants were lysed and

centrifuged to separate the cytosol and total membrane (TM) fractions. The fractions (10 μg protein each) were analyzed by IB using the indicated antibodies. PNS, postnuclear supernatant. (C) HeLa cells expressing Stx17ΔC-tail mutants were incubated with EBSS for 2 h and analyzed by IF microscopy (top). Scale bars, 10 μm. The bar graph on the bottom shows the quantification of LC3 dots positive for FLAG-tagged Stx17ΔC-tail mutants. Results are mean±s.e.m. from *n*=3 independent experiments. In each experiment, 30 cells were examined. *p < 0.05, ***p < 0.001. (D) HeLa cells expressing FLAG-tagged cStx17KKRA were analyzed by IF microscopy (top) and IB (bottom). PNS, postnuclear supernatant; TM, total membranes. Scale bars, 10 μm. (E) HeLa cells expressing FLAG-tagged dStx17K248A or cStx17A222K were starved for 2 h and analyzed by IF microscopy. Scale bars, 10 μm. In (B) and (D), molecular size markers (kDa) are shown.

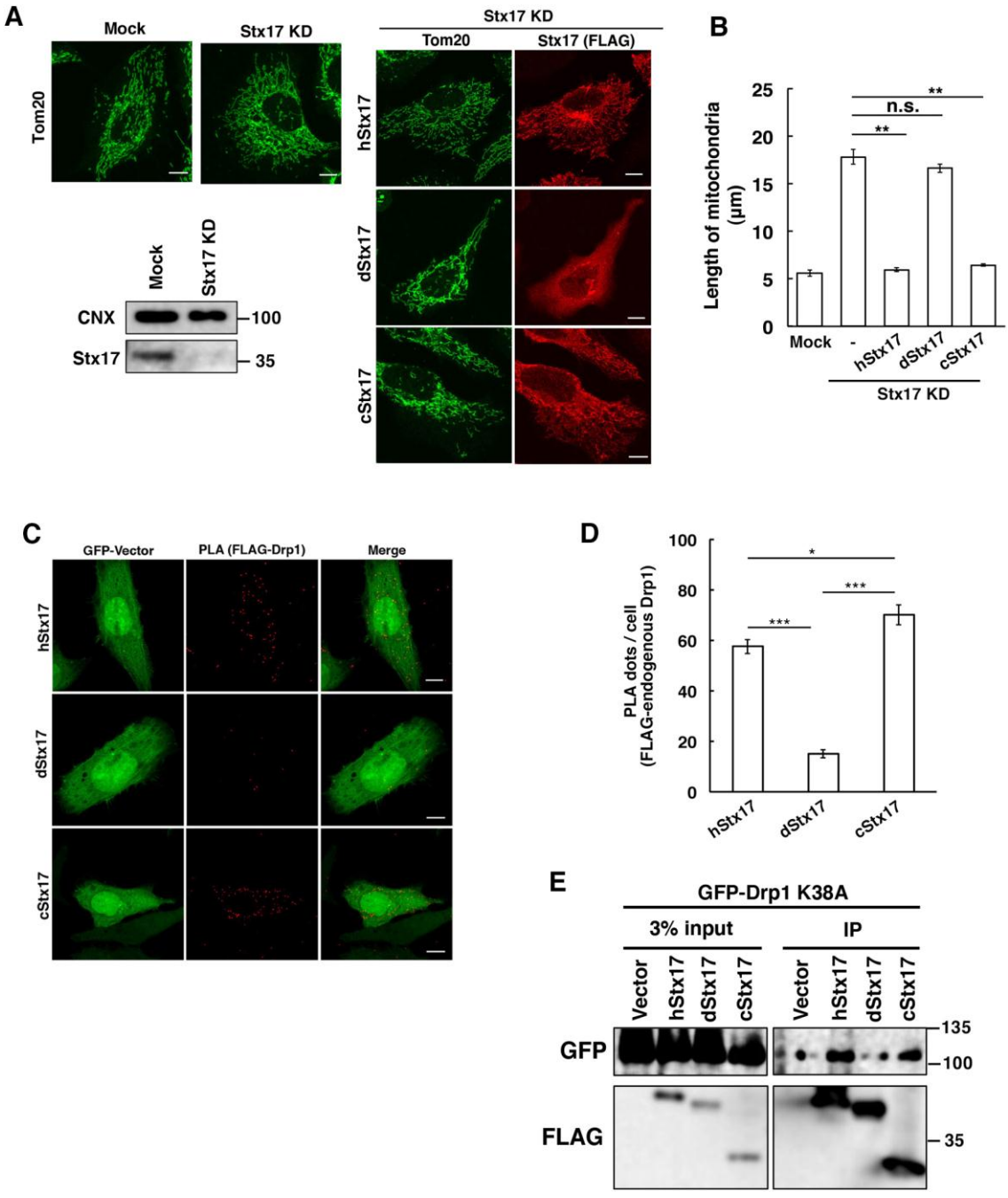

Fig. 3. cStx17 can compensate for the loss of hStx17 from HeLa cells with respect to mitochondrial division. (A) HeLa cells were mock treated or treated with siRNA Stx17 (3'-UTR) for 72 h (Stx17 KD). Alternatively, at 48 h after transfection of siRNA Stx17 (3'-UTR), cells were transfected with a plasmid encoding FLAG-tagged hStx17 (right, top row), dStx17 (right, middle row) or cStx17 (right, bottom row), further incubated for 24 h

and then double immunostained for Tom20 and FLAG. Scale bars, 10 μm. Bottom left panel shows the efficiency of Stx17 depletion. Cell lysates (10 μg protein each) were analyzed by IB using the indicated antibodies. (B) Quantification of the data in (A). Results are mean±s.e.m. from *n*=3 independent experiments. **p < 0.01, n.s., not significant. (C) HeLa cells were co-transfected with plasmids encoding GFP and FLAG-tagged hStx17 (top row), dStx17 (middle row) or cStx17 (bottom row). At 24 h after transfection, the cells were fixed and subjected to PLA analysis using antibodies against FLAG and Drp1. Scale bars, 10 μm. (D) Quantification of the data in (C). Results are mean±s.e.m. from *n*=3 independent experiments. *p < 0.05, ***p < 0.001. (E) 293T cells were co-transfected with plasmids encoding GFP-Drp1 K38A and FLAG-tagged Stx17. At 24 h after transfection, cell lysates were immunoprecipitated (IP) with anti-FLAG M2 beads, and analyzed by IB using antibodies against GFP and FLAG. Three percent of lysates was analyzed as input. In (A) and (E), molecular size markers (kDa) are shown.

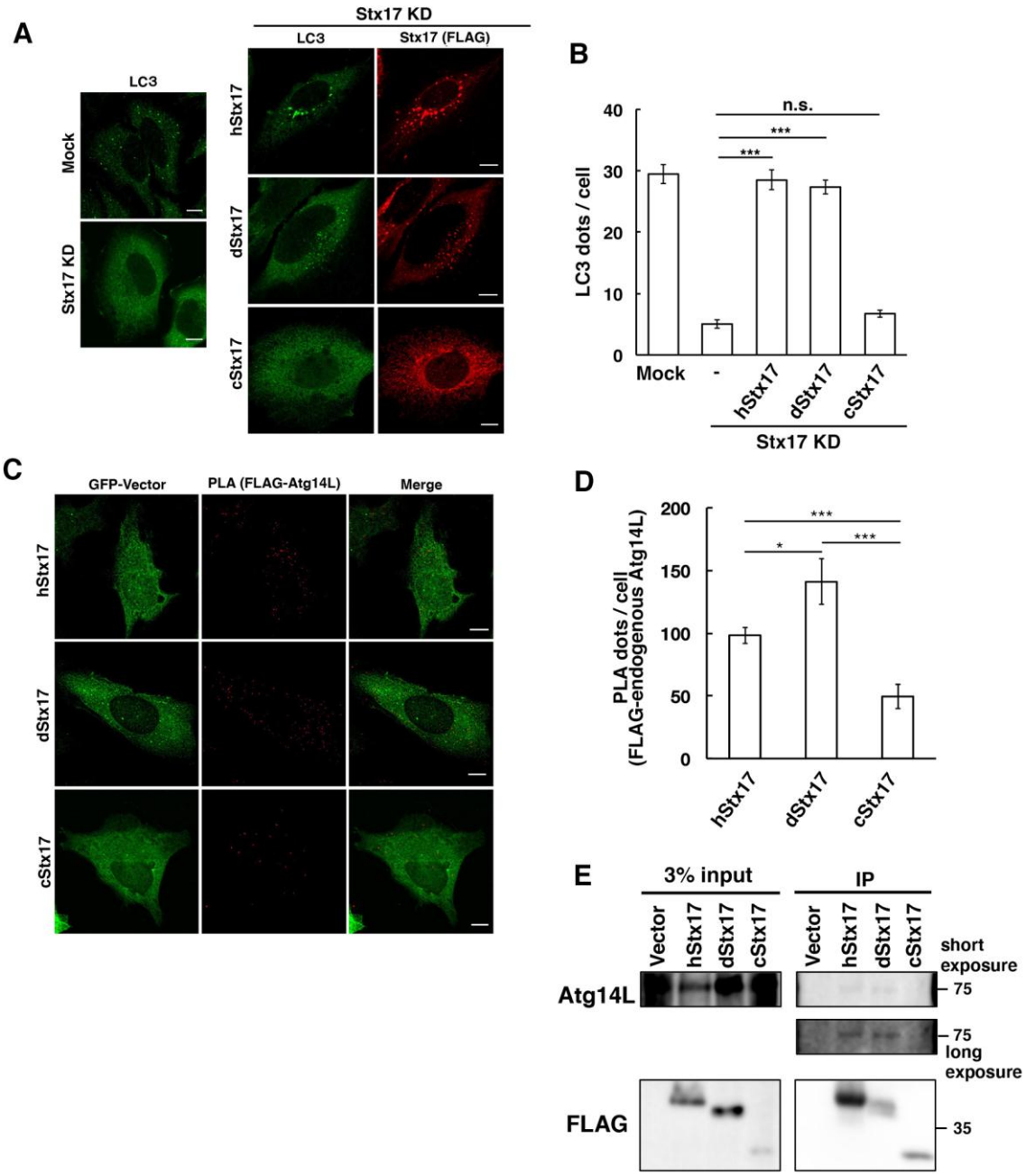

Fig. 4. dStx17 can compensate for the loss of hStx17 from HeLa cells with respect to autophagosome formation. (A) HeLa cells were mock treated (left, top row) or treated with siRNA Stx17 (3'-UTR) for 72 h (Stx17KD: left, bottom row). Alternatively, at 48 h after transfection of siRNA Stx17 (3'-UTR), cells were transfected with a plasmid encoding

FLAG-tagged hStx17 (right, top row), dStx17 (right, middle row) or cStx17 (right, bottom row), further incubated for 24 h. The cells were starved for 2 h and then double immunostained for LC3 and FLAG. Scale bars, 10 μm. (B) Quantification of the data in (A). Results are mean±s.e.m. from *n*=3 independent experiments. In each experiment, 30 cells were examined. ***p < 0.001, n.s., not significant. (C) HeLa cells were co-transfected with plasmids encoding GFP and FLAG-tagged hStx17 (top row), dStx17 (middle row) or cStx17 (bottom row). At 24 h after transfection, the cells were starved for 2 h, fixed and subjected to PLA analysis using antibodies against FLAG and Atg14L. Scale bars, 10 μm. (D) Quantification of the data in (C). D Results are mean±s.e.m. from *n*=3 independent experiments. *p < 0.05, ***p < 0.001. (E) 293T cells were transfected with a plasmid encoding FLAG-tagged Stx17. At 24 h after transfection, cell lysates were immunoprecipitated (IP) with anti-FLAG M2 beads, and analyzed by IB using antibodies against Atg14L and FLAG. Three percent of lysates was analyzed as input. Molecular size markers (kDa) are shown.

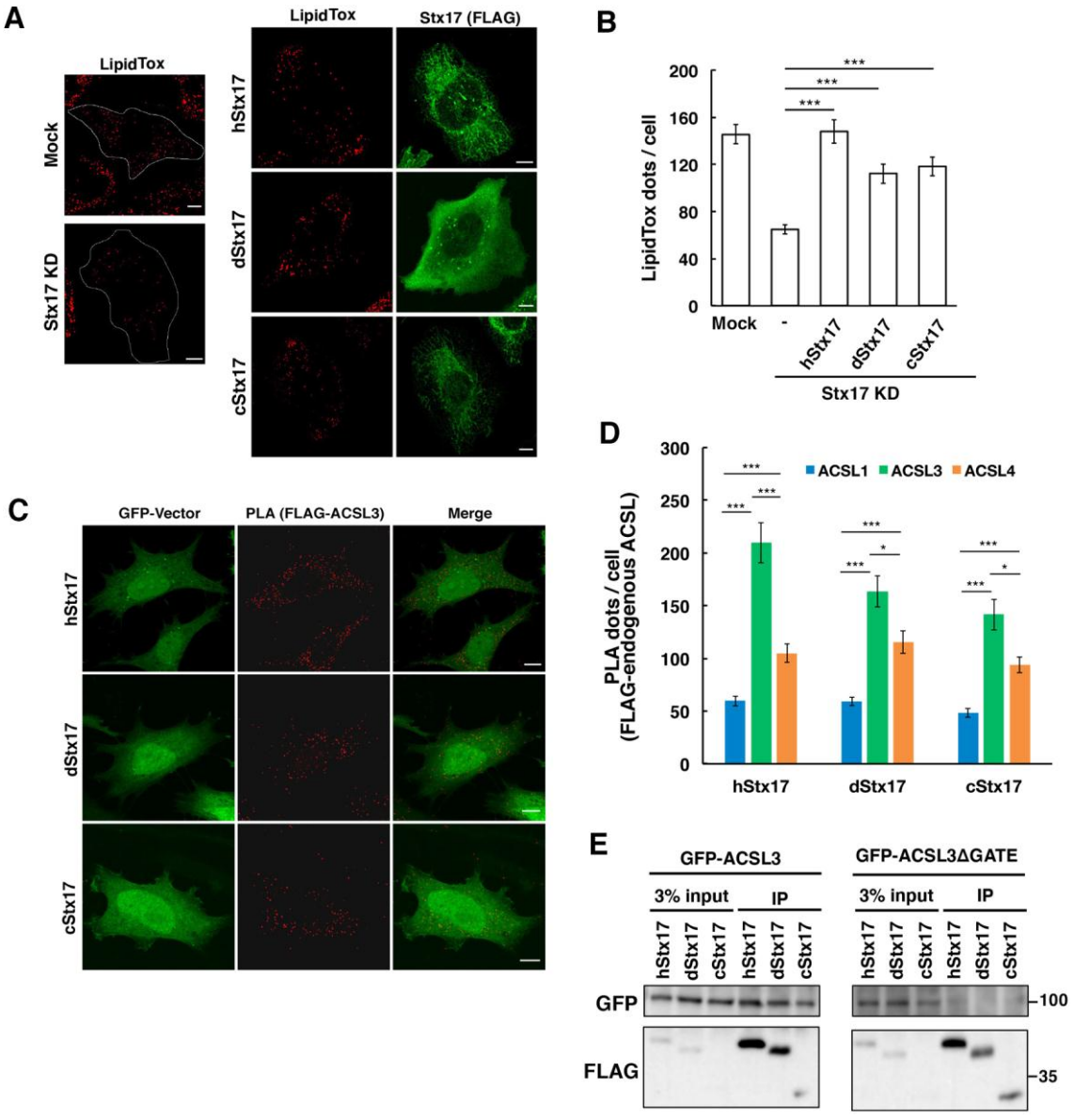

Fig. 5. Both dStx17 and cStx17 can interact with ACSL3 and promote lipid droplet formation. (A) HeLa cells were mock treated (left, top row) or treated with siRNA Stx17 (3'-UTR) for 72 h (Stx17KD: left, bottom row). The cells were incubated with 150 μM oleic acid-BSA for the last 16 h, and stained with LipidTox to visualize lipid droplets. Alternatively, at 48 h after transfection of siRNA Stx17 (3'-UTR), cells were transfected with a plasmid encoding FLAG-tagged hStx17 (right, top row), dStx17 (right, middle row)

or cStx17 (right, bottom row), incubated with oleic acid and stained with LipidTox. Scale bars, 10 μm. (B) Quantification of the data in (A). Results are mean±s.e.m. from *n*=3 independent experiments. In each experiment, 30 cells were examined. ***p < 0.001. (C) HeLa cells were co-transfected with plasmids encoding GFP and FLAG-tagged hStx17 (top row), dStx17 (middle row) or cStx17 (bottom row). At 24 h after transfection, the cells were fixed and subjected to PLA analysis using antibodies against FLAG and ACSL 1, 3 or 4. Images only for FLAG-ACSL3 PLA are shown. Scale bars, 10 μm. (D) Quantification of the data in (C). Blue, green and orange bars represent proximity signals between Stx17 and ACSL1, 3 and 4, respectively. Results are mean±s.e.m. from *n*=3 independent experiments. *p < 0.05, ***p < 0.001. (E) 293T cells were co-transfected with plasmids encoding FLAG-tagged Stx17and GFP-ACSL3 (left) or GFP-ACSL3ΔGATE (right). At 24 h after transfection, cell lysates were immunoprecipitated (IP) with anti-FLAG M2 beads, and analyzed by IB using antibodies against GFP and FLAG. Three percent of lysates was analyzed as input. Molecular size markers (kDa) are shown.

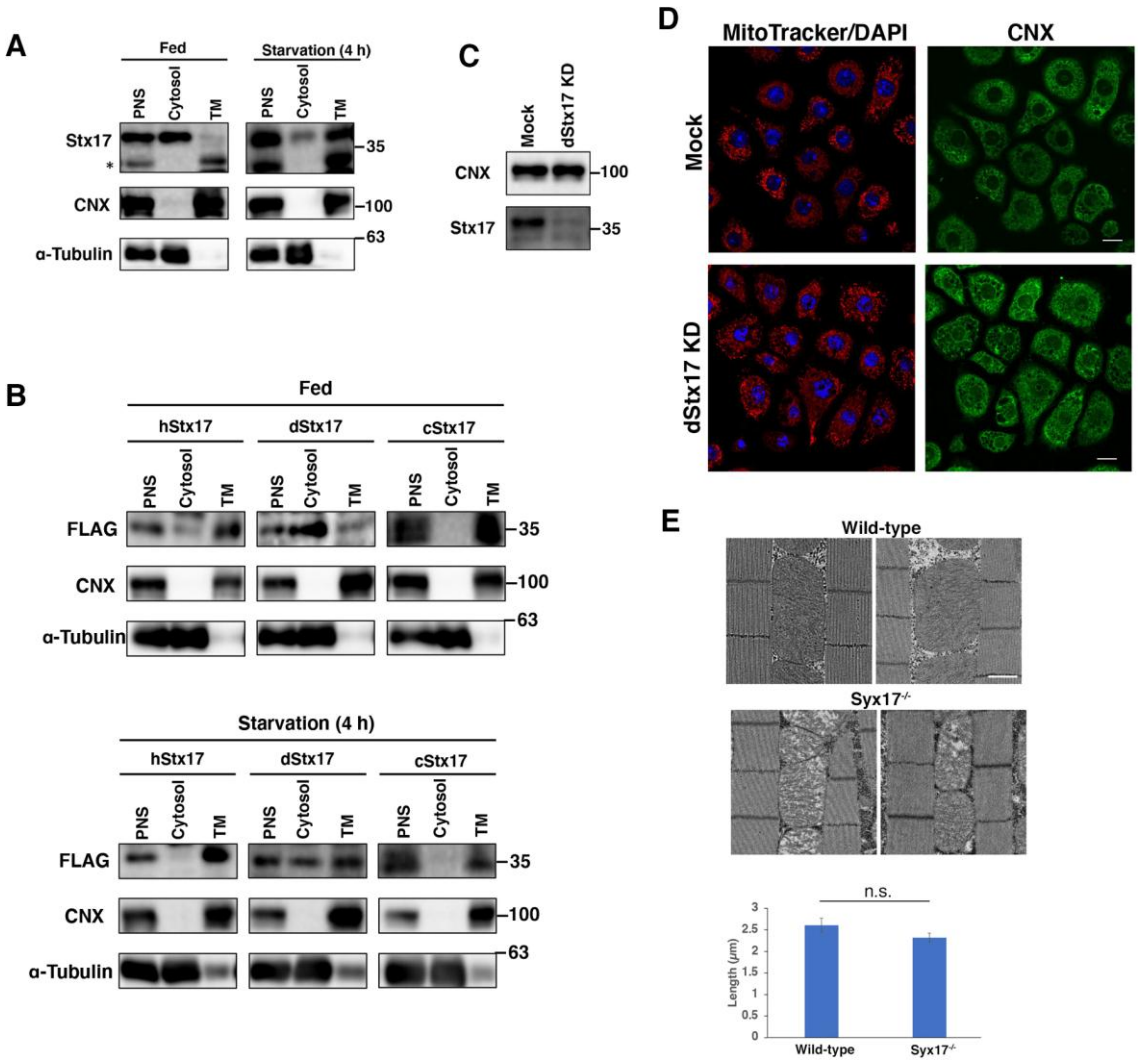

Fig. 6. dStx17 mainly localizes to the cytosol and does not participate in mitochondrial division. (A) S2 cells without or with starvation treatment for 4 h were lysed and centrifuged to separate the cytosol and total membrane (TM) fractions. The fractions (10 μg protein each except that 1 μg protein was used for α-tubulin detection) were analyzed by IB using the indicated antibodies. PNS, postnuclear supernatant. (B) S2 cells expressing each Stx17 construct were lysed and centrifuged as described in (A). The fractions (10 μg protein each except that 2 μg protein was used for α-tubulin detection) were analyzed by IB using the indicated antibodies. (C) S2 cells were mock-treated or transfected with siRNA for 72 h (dStx17 KD), and then triple-stained with DAPI and MitoTracker Red CMXRos (left) and

anti-CNX (right). Bar, 10 μm. (E) Transmission electron microscopy images of the indirect flight muscle. Two typical images are shown for wild-type and *Syx17*$^{-/-}$, respectively. Bar, 1 μm. The bar graph shows the quantification of the length of the mitochondrial long axis. Results are mean±s.e.m. from *n*=31 (wild-type) or 71 (*Syx17*$^{-/-}$) mitochondria from three flies. n.s., not significant. In (A), (B) and (C), molecular size markers (kDa) are shown.

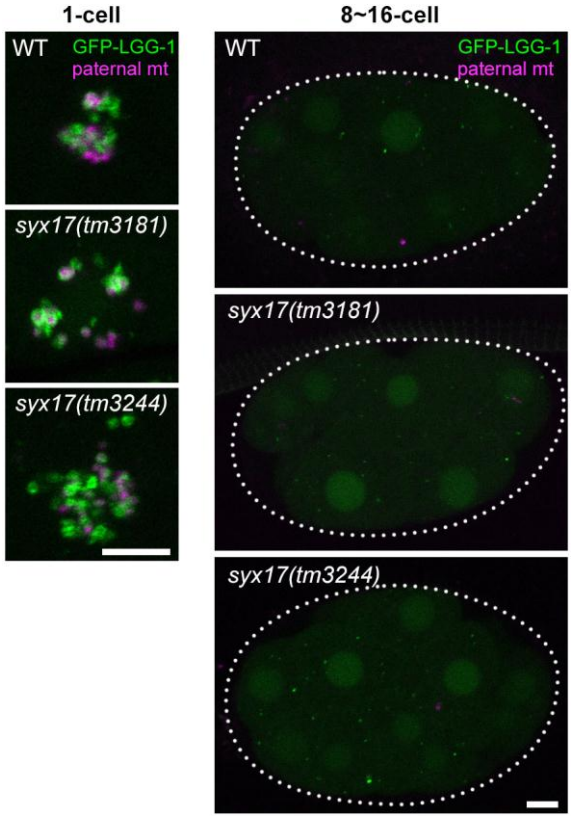

Fig. 7. Allophagy in *C. elegans* embryos is not affected by *syx17* mutations. GFP-LGG-1 (green) and paternal mitochondria (HSP-6-mCherry; magenta) were observed in 1-cell-stage or 8-16-cell stage embryos of the wild-type and the indicated *syx17* mutant strains. Bars, 5 μm.

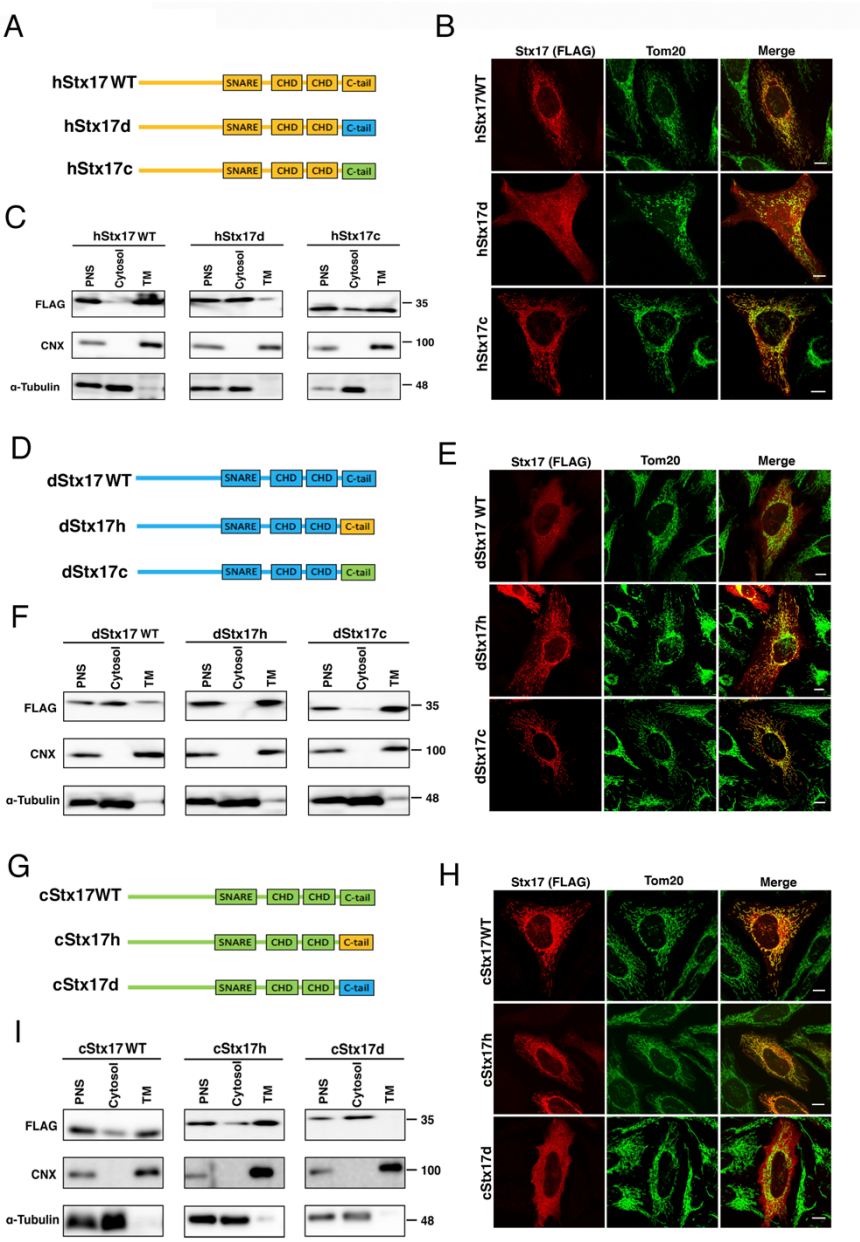

Fig. S1. Localization of Stx17 chimeras in HeLa cells. (A,D,G) Schematic representation of Stx17 chimeras. The regions corresponding to human, fly and nematode Stx17 species are shown in yellow, right blue and yellow green, respectively. (B,E,H) HeLa cells were transfected with a plasmid encoding each chimera. At 24 h after transfection, the cells were fixed and analyzed by IF microscopy. Scale bars, 10 µm. (C,F,I) HeLa cells expressing each Stx17 chimera were lysed and centrifuged to separate the cytosol and total membrane (TM) fractions. The fractions (10 µg protein each) were analyzed by IB using the indicated antibodies. PNS, postnuclear supernatant. In (C), (F) and (I), molecular size markers (kDa) are shown.

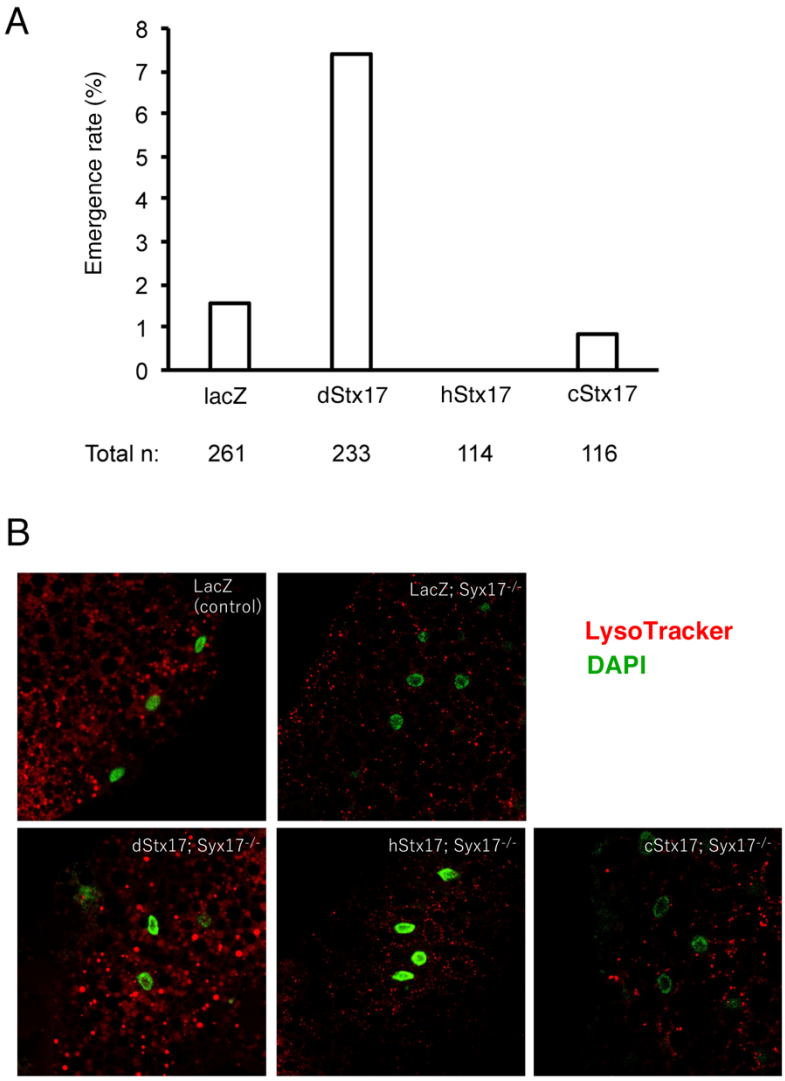

Fig. S2. Neither hStx17 nor cStx17 can compensate for the function of dStx17 in vivo. (A) The total number of offspring and the percentage of *Syx17*$^{LL06330/LL06330}$ offspring obtained by crossing *Act5C-GAL4/CyO-GFP; Syx17*^{LL06330}*/TM6B* with *UAS-LacZ/CyO-GFP; Syx17*^{LL06330}*/TM6B* (LacZ), *UAS-dStx17/CyO-GFP; Syx17*^{LL06330}*/TM6B* (dStx17), *UAS-hStx17/CyO-GFP; Syx17*^{LL06330}*/TM6B* (hStx17) or *UAS-cStx17/CyO-GFP; Syx17*^{LL06330}*/TM6B* (cStx17). (B) LysoTracker staining of the fat body in the third instar larva starved for 3 h. Nuclei were counterstained with DAPI. Genotypes used were as follows: *Act5C-GAL4/UAS-LacZ* (LacZ), *Act5C-GAL4/UAS-LacZ; Syx17*^{LL06330}*/Syx17*^{LL06330} (LacZ; Syx17$^{-/-}$), *Act5C-GAL4/UAS-dStx17; Syx17*^{LL06330}*/Syx17*^{LL06330} (dStx17; Syx17$^{-/-}$), *Act5C-GAL4/UAS-hStx17; Syx17*^{LL06330}*/Syx17*^{LL06330} (hStx17; Syx17$^{-/-}$), *Act5C-GAL4/UAS-cStx17; Syx17*^{LL06330}*/Syx17*^{LL06330} (cStx17; Syx17$^{-/-}$). Scale bar, 50 µm.